VERIFICATION, VALIDATION AND APPLICATION OF NEPTUNE_CFD TO TWO-PHASE PRESSURIZED THERMAL SHOCKS

N. Mérigoux, J. Laviéville, S. Mimouni, M. Guingo and C. Baudry
Electricité de France, R&D Division
6 Quai Watier, 78401 Chatou, France
nicolas.merigoux@edf.fr

S. Bellet

Electricité de France, Thermal & Nuclear Studies and Projects Division
12-14 Avenue Dutriévoz, 69628 Villeurbanne, France
serge.bellet@edf.fr

ABSTRACT

Nuclear Power Plants are subjected to a variety of ageing mechanisms and, at the same time, exposed to potential Pressurized Thermal Shock (PTS) – characterized by a rapid cooling of the Reactor Pressure Vessel (RPV) wall. In this context, NEPTUNE_CFD is developed and used to model two-phase PTS in an industrial configuration, providing temperature and pressure fields required to assess the integrity of the RPV. Furthermore, when using CFD for nuclear safety demonstration purposes, EDF applies a methodology based on physical analysis, verification, validation and application to industrial scale (V&V), to demonstrate the quality of, and the confidence in results obtained. By following this methodology, each step must be proved to be consistent with the others, and with the final goal of the calculations. To this effect, a chart demonstrating how far the validation step of NEPTUNE_CFD is covering the PTS application will be drawn. A selection of the code verification and validation cases against different experiments will be described. For results consistency, a single and mature set of models – resulting from the knowledge acquired during the code development over the last decade – has been used. From these development and validation feedbacks, a methodology has been set up to perform industrial computations. Finally, the guidelines of this methodology based on NEPTUNE_CFD and SYRTHES coupling – to take into account the conjugate heat transfer between liquid and solid – will be presented. A short overview of the engineering approach will be given – starting from the meshing process, up to the results post-treatment and analysis.

1. INTRODUCTION

Nuclear Power Plants (NPP) operating equipments are subjected to a variety of ageing mechanisms. Ageing effects of the Reactor Pressure Vessel (RPV) have the potential to be a lifetime-limiting condition for a NPP as the RPV is impossible or economically unviable to replace. Pressurized Thermal Shock (PTS) transient is characterized by a rapid cooling (i.e. thermal shock) of the downcomer and internal RPV surface, followed sometimes by re-pressurization of the RPV. Thus, a PTS event raises a potentially significant challenge to the structural integrity of the RPV in a Pressurized Water Reactor (PWR). In this context, NEPTUNE_CFD is developed – within the framework of the NEPTUNE project [1] - and used

to model two-phase PTS in an industrial configuration, providing temperature and pressure fields required to assess the integrity of the RPV.

Furthermore, when using CFD for nuclear safety demonstration purposes, EDF applies a methodology based on physical analysis, verification, validation and application to industrial scale (V&V), to demonstrate the quality of, and the confidence in results obtained. By following this methodology, each step must be proved to be consistent with the others, and with the final goal of the calculations. The physical analysis, based on a PIRT (Phenomena Identification and Ranking Table) dedicated to the specific CFD scenario, has a key role to achieve this consistency [2]. To this effect, a chart demonstrating how far the validation step is covering the PTS application will be drawn prior to apply NEPTUNE_CFD on an industrial scenario.

This paper will also describe a selection of the code validation against different experiments which have been selected to allow separated effects and integral validations. To add some confidence in the validation results, a verification step has first been performed on some very simple cases. All this work has been done following the existing best practice guidelines and a mesh refinement analysis has been carried out during all the V&V process. For results consistency, a single and mature set of models – resulting from the knowledge acquired during the code development over the last decade – has been used and will be briefly described.

From these development and validation feedbacks, a methodology has been set up to perform industrial computations. This paper will present the guidelines of this methodology based on NEPTUNE_CFD and SYRTHES coupling – to take into account the conjugate heat transfer between liquid and solid. A short overview of the engineering approach will be given – starting from the meshing process, up to the results post-treatment and analysis.

2. MODEL DESCRIPTION

The purpose of this paper being to present the validation and application of NEPTUNE_CFD 3.0 in a PTS context, the following section will only describe the main principles of the used models – without any details on the governing equations. Next sections will be dedicated to the verification and validation steps.

2.1. Two-phase model and solver

NEPTUNE_CFD is a three dimensional two-fluid code developed more especially for nuclear reactor applications. This code is based on the classical two-fluid one-pressure approach [3-4], and is able to simulate multi-component multiphase flows by solving a set of three balance equations for each field [1, 5-7]. These fields can represent many kinds of multiphase flows: distinct physical components (e.g. gas, liquid and solid particles); thermodynamic phases of the same component (e.g. liquid water and its vapour); distinct physical components, some of which split into different groups (e.g. water and several groups of different bubble diameters); different forms of the same physical components (e.g.: a continuous liquid field, a dispersed liquid field, a continuous vapour field, a dispersed vapour field).

The discretisation follows a 3D full-unstructured finite-volume approach, with a collocated arrangement of all variables. Numerical consistency and precision for diffusive and advective fluxes for non-orthogonal and irregular cells are taken into account through a gradient reconstruction technique. Convective schemes for all variables, except pressure, are centred / upwind scheme. Velocities components can be computed with a full centred scheme. The solver is based on a pressure correction fractional step approach. Gradients are calculated at second order for regular cells and at first order for highly irregular cells.

A set of local balance equations for mass, momentum and energy is written for each phase. These balance equations are obtained by ensemble averaging of the local instantaneous balance equations written for each phase. When the averaging operation is performed, the major part of the information about the interfacial configuration and the microphysics governing the different types of exchanges is lost. As a consequence, a number of closure relations must be supplied for the total number of equations (the

balance equations and the closure relations) to be equal to the number of unknown fields. We can distinguish three different types of closure relations. Those which express the inter-phase exchanges (interfacial transfer terms), those which express the intra-phase exchanges (molecular and turbulent transfer terms) and those which express the interactions between each phase and the walls (wall transfer terms) [7].

2.2. Large Interface Model

Two-phase PTS CFD scenarios involve interfaces between liquid and vapour which are generally much larger than the computational cells size: the "large interfaces". Specific models to deal with them were developed and implemented in NEPTUNE_CFD: it is the Large Interface Model (LIM) [8]. It includes large interface recognition, interfacial transfer of momentum (friction), heat and mass transfer with Direct Contact Condensation (DCC). The LIM takes into account large interfaces which can be smooth, wavy or rough.

Regarding the interface recognition, the method implemented in NEPTUNE_CFD is based on the gradient of liquid fraction. The first step consists in computing a refined liquid fraction gradient, based on harmonic or anti-harmonic interpolated values of liquid fraction on the faces between the cells [9]. This refined gradient allows us to detect the cells belonging to the Large Interface (LI). The models – specific LI's closure laws – developed and implemented in NEPTUNE_CFD [10-12] are written within a three-cell stencil (LI3C) around the large interface position (including the two liquid and vapour neighbouring cells located in LI's normal direction). This stencil is used to compute, on both the liquid and gas sides, the distance from the first computational cell to the large interface. Both distances are used in the models written in a wall law-like format. In this manner, only physically relevant values are used by choosing the interface side where the phase is not residual and the effect of the LI's position with regard to the mesh is limited.

2.3. Turbulence model

Several turbulence models are available in NEPTUNE_CFD to solve all kind of high-Reynolds multiphase flows. Regarding free surface flows, classical models like k-ε [13] or k-ε "linear production" [14] where available in previous versions. A more advanced Reynolds Stress turbulence Model, namely R_{ij}-ε SSG [15], has been introduced recently to model highly anisotropic turbulence that is encountered in PWR. Indeed, based on the feedback acquired on solving single phase flows and two-phase bubbly flows [16], the choice has been made to first implement the R_{ij}-ε SSG model that has first been introduced by Speziale et al. [15]. Regarding the interface treatment of the turbulence and its integration within the LIM, a wall law-like format has been adopted, as already done for the k-ε model [17].

As a first step in applying RSM into the PTS context, the choice of the R_{ij}-ε SSG turbulence model seems to be a good compromise between short-terms developments and the need to get a quick and general tendency on various PTS related test cases. Coupled with the Large Interface Model, the first results confirmed the adequacy and accuracy of the approach to deal with adiabatic or thermal free surface flows [18-19].

3. CFD CODE VALIDATION PROCESS

For any scientific approach and particularly for simulations, it must be rigorous and necessary, for the acceptance, to well define a methodology through objective: decide whether a code may be used to compute quality-controlled industrial applications, or may be used with caution considering specific physics, or may be used only after working further on validation. This objective is one important step in accepting studies dedicated to the safety demonstration of nuclear power plants.

3.1. The key role of the PIRT for code validation process

In this Safety context, EDF is currently working with a specific VVUQ (Verification, Validation & Uncertainty Quantification) methodology for CFD applications, where the PIRT (Phenomena Identification Ranking Table) plays a key role (see Figure 1).
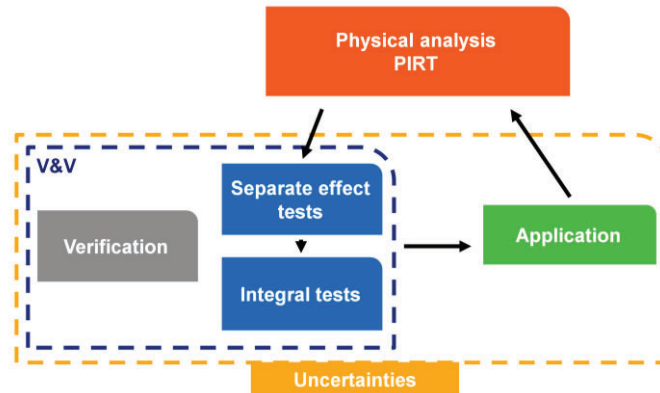

Figure 1. VVUQ methodology for CFD applications

PIRT is a formal method, supporting the classical engineer analysis, well described in many papers [20-21]. Understanding of the involved physical phenomena to have a V&V process consistent with application domain comes from this fundamental step. As it is an iterative process one can start with an expert's assessment and complete during the following iterations with some sensitivity studies to refine the PIRT conclusions. To describe more precisely the PIRT process one can tackle it according to the following steps:

- Define the problem.
- Define the PIRT objective.
- Identify the studied transient.
- Identify parameters of interest or dominant parameters (Figures of Merits – FoM) and desired accuracy.
- Identify Physical phenomena (and associated parameters for a more accurate PIRT).
- Rank by importance the influence and knowledge level of different parameters on FoM, to get a trustworthy index.
- Deliver a PIRT table.

One can add that, if one usually uses a PIRT for code evaluation, the PIRT is also commonly used for experiments, design, code development and new system definition strategy. The PIRT table is thus complete with the level of knowledge of the phenomena or parameters. Consequently, it can be very useful to guide decision makers, to get to the point. Based on this PIRT the V&V process can be executed.

3.2. V&V process: representing application and validation domains

The word "domain" expresses a need of a visual representation with easy understanding, where one can point out overlapping, interpolations or extrapolations between "domains". In other words, this is a need to get confidence for application studies based on validation exercise (see Figure 1). Based on the PIRT analysis, an application domain can be defined. For that, an additional element is needed: the dimensionless numbers combining the main parameters to quantify the physical phenomena identified.
The template of the chart (see Figure 2) must represent the three bases of the physical analysis: figures of merits, main physical phenomena and associated dimensionless numbers. More details on how to build it are related in [2].

3.3. Application to two-phase PTS

The objective here is to represent the validation domain of NEPTUNE_CFD 3.0 regarding the two-phase PTS application, and see how it is positioned with regard to the industrial application. For that purpose a complete list of the validation cases of NEPTUNE_CFD 3.0, dedicated to the PTS application is drawn hereafter (Table I). The main physical phenomena are issued from a PIRT analysis dedicated to two-phase PTS:

- Ph. 1: Jet impact on free surface and wall (including injection pipe dewatering)
- Ph. 2: Interfacial transfer of heat & mass
- Ph. 3: Interfacial transfer of momentum
- Ph. 4: Thermal stratification
- Ph. 5: Flow curvature and buoyancy plume oscillations

Table I. Separate effect and integral (*in italic*) validation cases of NEPTUNE_CFD for the two-phase PTS application

Experiment	Ph. 1	Ph. 2	Ph. 3	Ph. 4	Ph. 5	Dimensionless numbers (Re / Fr)	Comments
Maschek et al. (1992)			X			4.10^4 / > 1	Liquid sloshing in a pool - 1 test case: unsteady flow
Kleefsman et al. (2006)			X			7.10^5 / > 1	3D dambreaking impacting a tank - 1 test case: unsteady flow
US Corps of Engineers (1990)			X			$5.5\ 10^5$ / 0.35	Free surface flow over a creager spillway - 1 test case: turbulent steady flow
Fabre et al. (1987)			X			$[1.10^4\ ;\ 5.10^4]$ / 0.02	Cocurrent air / water stratified channel - 2 test cases: turbulent smooth flows
Lim et al. (1984)		X				$[1.10^3\ ;\ 1.10^4]$ / 0.02	Cocurrent steam / water stratified channel - 8 test cases: turbulent smooth to wavy flows
Chu et al. (2000 - 2006)		X	X	X		$[4.10^3\ ;\ 2.10^4]$ / 0.34	Counter-current steam / water stratified channel - 8 test cases: turbulent smooth to wavy flows
Lee et al. (2015)		X	X	X		$1.5\ 10^3$ / 0.1	Cocurrent air or steam / water stratified channel - 6 test cases: turbulent smooth to wavy flows (3 air / water & 3 steam / water)
Kawamura et al. (1998)				X		$2.7\ 10^4$ / > 1	DNS of a single phase turbulent heat transfer in channel flow - 8 test cases with varying Pr numbers
Iguchi et al. (1997)	X					$1.3\ 10^4$ / Not defined	Dynamics below a vertical plunging liquid jet - 2 test cases: single-phase and two-phase flows
Bonetto and Lahey (1993)	X					$4.5\ 10^4$ / Not defined	Air entrainment by a vertical plunging liquid jet - 1 air / water test case
Hager (1998)	X					$4.3\ 10^5$ / [0.6 ; 1.2]	Cavity outflow from an horizontal pipe - 6 air / water test cases
Brison and Brun (1991)	X					$2.3\ 10^4$ / Not defined	Vertical jet impingement on a flate plate - 1 test case: thermal heating by the wall of a single phase jet
Péniguel and Hecker (1991)				X		$1.3\ 10^4$ / 0.02	Thermally stratified T-junction - 1 test case: thermal stratification of a single phase flow
HYBISCUS II	*X*		*X*	*X*	*X*	*$[5.10^4\ ;\ 1.10^5]$ / [0.2 ; 1]*	*Half of a PWR 1300 MWe primary circuit scale ½ - 3 test cases: single-phase and two-phase flows, with and without natural flow circulation in cold legs*
UPTF	*X*	*X*	*X*	*X*	*X*	*$[5.10^4\ ;\ 5.10^5]$ / [0.1 ; 1.8]*	*PWR 1300 MWe primary circuit scale 1 - 1 single-phase and 1 two-phase flows with conjugate heat transfer*
COSI	*X*	*X*	*X*	*X*	*X*	*$[3.10^3\ ;\ 2.10^4]$ /*	*Cold leg of a PWR 900 MWe scale 1/100 - 3*

						[0.04 ; 1.7]	test cases of steam / water flows with varying water layer heights
TOPFLOW-PTS	X	X	X	X	X	[1.10⁴ ; 5.10⁴] / [0.1 ; 1]	Cold leg and downcomer of a PWR 900 MWe scale 1/2.5 - 7 steady state test cases of steam / water flows with varying water layer heights and ECC mass flow rates + 1 transient steam / water case

From this table, the chart representing the figure of merit (wall temperature and heat transfer coefficient), the main physical phenomena and the associated dimensionless numbers is drawn (Figure 2):

Figure 2. Validation and application domains of NEPTUNE_CFD for two-phase PTS

From the PIRT analysis and this chart we can clearly see that the overall validation of NEPTUNE_CFD does cover a great part of the targeted application domain. Nevertheless we can also point out that there is still a lack of separated effects validation for the flow curvature and buoyancy plume oscillations physical phenomenon. This point will have to be investigated during the next validation process as there might be some experiments available to validate this phenomenon – at least for single phase flows.

4. VERIFICATION CASES

To add some confidence in the recent developments and prior to the computation of various validation cases, a verification step has been performed on some very simple 1D periodic stratified channel flows. It mainly allows us to verify the velocity and turbulence fields' behaviour near the boundaries and at the interface. Only one case, dealing with a two-phase laminar channel flow, will be described here. Other cases have been developed to verify the turbulence fields' behaviour and are available in [18].

4.1. Description of the test case

A one-dimensional, laminar, two-phase channel flow is simulated: a liquid phase is flowing at the bottom part of the domain with a mean velocity equal to U_1. Above the liquid flow, a co-current gas flows with a velocity equal to U_2. The two phases are set into motion through the use of momentum source terms corresponding to the analytical expression of the pressure gradient – the pressure is not explicitly

computed. The two phases are incompressible and isothermal. The flow is considered laminar; hence no turbulence modelling is needed. The effect of gravity is not taken into account. A sketch of the test-case principle is represented in Figure 3.
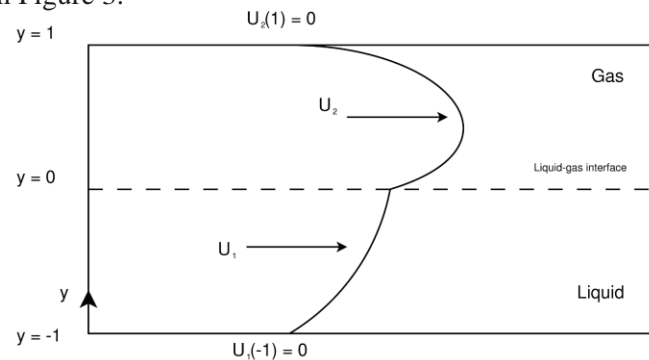

Figure 3. Two-phase channel flow verification case

The test case is useful to investigate the shear-stress computation through a free surface, and consequently to validate the numerical methods of the LIM. In this configuration, the stratified flow can be assimilated as a "double" plane Poiseuille flow. It is then possible to calculate an analytical solution for the velocity fields of both phases.

4.2. Computational representation

For this case, the influence of the position of the free-surface – with regard to the channel discretisation – is investigated. Therefore, two meshes are used (see Table II): one where the interface is located between two mesh cells (Grid level 1), another one with a slightly different refinement where the interface is crossing a mesh cell (Grid level 2). As the solution is 1D, there is only one cell in the two space directions that are tangential to the free surface. These meshes involve orthogonal and hexahedral cells only.

Table II. Mesh refinements for the verification case

Grid	Number of cells
Level 1	400
Level 2	401

4.3. Results

The velocity profiles for the two phases and the two meshes are shown in Figure 4. It is observed that the theoretical solution is satisfactorily retrieved by NEPTUNE CFD and that the influence of the free-surface position – with regard to the mesh refinement – is negligible.
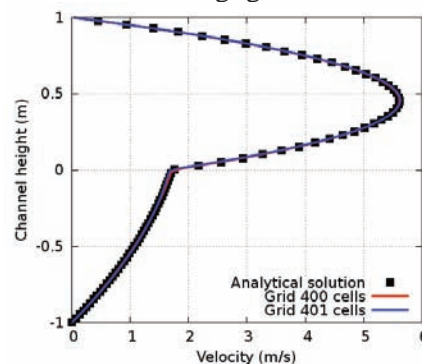

Figure 4. Velocity profiles of the two-phase channel flow

5. VALIDATION ON SEPARATE EFFECT CASES

The following section will now focus on separated effects validation. To do this, a selection of flows encountered in PTS scenarios will be studied. For the sake of brevity, only a few cases issued from the physical analysis will be described. This part will be dedicated to two-phase stratified flows that may take place in a part of the cold leg, as well as more complex turbulent two-phase flow configurations. Indeed, Eulerian two-phase code calculations of PTS require a correct modelling of heat and mass transfer on free surfaces, which directly depends on turbulence in both liquid and gas, which in return depends on interfacial transfer of momentum. The most important parameters from the PTS point of view are horizontal averaged velocities and turbulent kinetic energy on the liquid side.

The modelling difficulties will increase gradually by starting with isothermal flows which do not require any turbulence modelling, up to turbulent flows with heat and mass transfers.

5.1. Free surface flows dynamics

5.1.1. Description of the test case

The 3D dambreaking test case, based on Kleefsman et al. experiment [22] is used to validate the free surface dynamics modelling. In this experiment, a large tank of 3.22 m long, 1 m wide and 1 m high is used with an open roof. The right part of the tank is first closed by a door. Behind the door, 0.55 m of water is waiting to flow into the tank when the door is opened. This is done by releasing a weight, which almost instantaneously pulls the door up. In the tank, a box has been placed that represents a scale model of a container on the deck of a ship. During the experiment, measurements have been performed on water heights, pressures and forces. As shown in Figure 5, four vertical height probes have been used: one in the reservoir and the other three in the tank. The box was also covered by eight pressure sensors, four on the front of the box and four on the top.
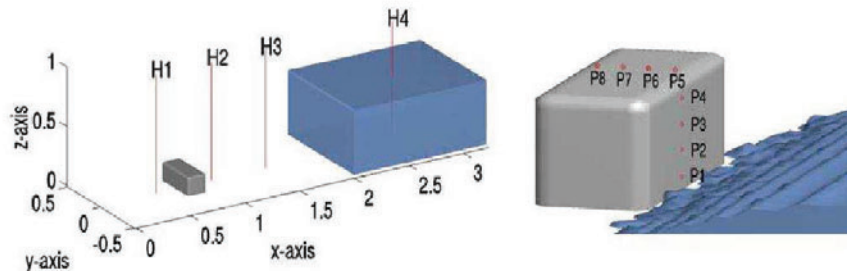

Figure 5. Measurement positions for water heights and pressures in the dambreak experiment

5.1.2. Computational representation

To determine the sensibility to the mesh refinement, three levels of grid have been used (see Table III), with a constant cell length in the three spatial directions. We considered a two-phase, isothermal and laminar flow, with constant densities and viscosities.

Table III. Hierarchy of refined meshes for the 3D dambreaking experiment

Grid	Number of cells
Level 1	43 136
Level 2	375 920
Level 3	3 007 360

5.1.3. Results

Figure 6 and Figure 7 show the calculations results and their comparisons with the experimental data. The top graphs present the water heights within the tank while the wave is flooding the reservoir. The other graphs show the pressure that is applied on the reservoir while the water wave is breaking. Calculation results (lines) are compared with the experiment (black symbols) for the three mesh refinements.
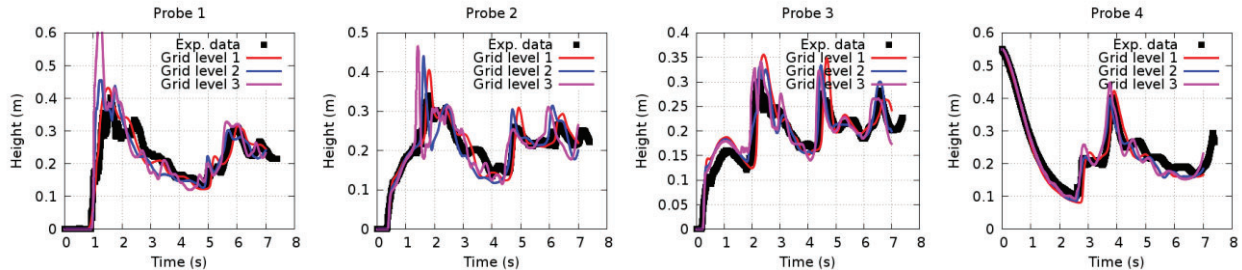

Figure 6. Water heights at the four probes positions – comparison between experiment data (symbols) and NEPTUNE_CFD (continuous lines)
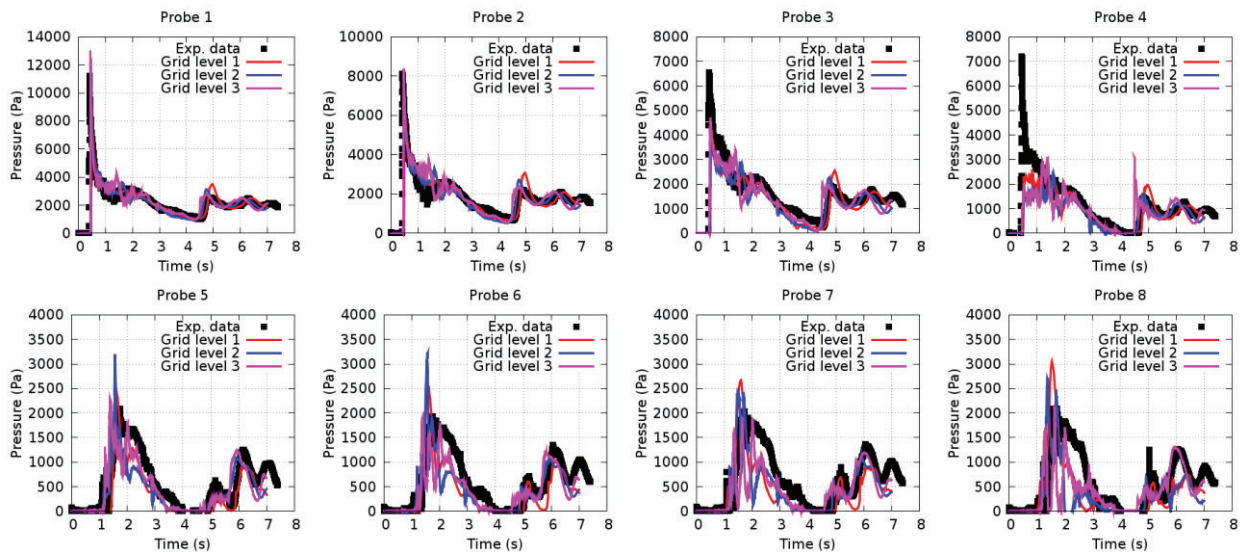

Figure 7. Relative pressures at the height probes positions – comparison between experiment data (symbols) and NEPTUNE_CFD (continuous lines)

Water heights within the tank are overall well predicted. The maximum heights of some waves are sometimes overestimated (see Probe 1 of Figure 6) but this might be due to the way results are post-treated – numerically the liquid fraction will tend to increase as much as we refine in these areas where a singularity occurs, while experimentally the presence of detaching droplets may not be catch by the probes. The conclusions remain the same for the pressure predictions. The worst agreement is observed at Probe 4 where a flow separation is taking place.

Eventually, the agreement (waves and pressure peaks are predicted with a good timing) and the weak sensitivity to the mesh refinement are satisfactory. It gives confidence before adding turbulence into the free surface modelling.

5.2. Air / water stratified flows in a channel

5.2.1. Description of the test case

The Air / Water STratified (AWST) test case, based on the Fabre et al. experiment [23] is used to validate the dynamic part of the LIM, in terms of momentum and turbulent energy transfers at the free surface. It is an adiabatic air water co-current stratified flow, in a 12 m long, 20 cm wide, 10 cm high and 0.1 % bottom slope. The inlet liquid superficial velocity is 0.15 m/s, which corresponds to a water flow rate equal to 3 l/s. Our selected test is the run 250, where the inlet gas superficial velocity (2.5 m/s) is high enough for the interfacial friction to play an important role, and sufficiently weak for waves to be negligible. In this run, the Reynolds number (19 000) is large enough to validate the use of the turbulence model. The water height is set to 3.8 cm. The measurements used for the CFD comparisons are done at 9.1 m from the inlet, on a vertical line in the channel axis. Vertical profiles are obtained for gas and liquid horizontal velocities, turbulent kinetic energy and turbulent shear stress.
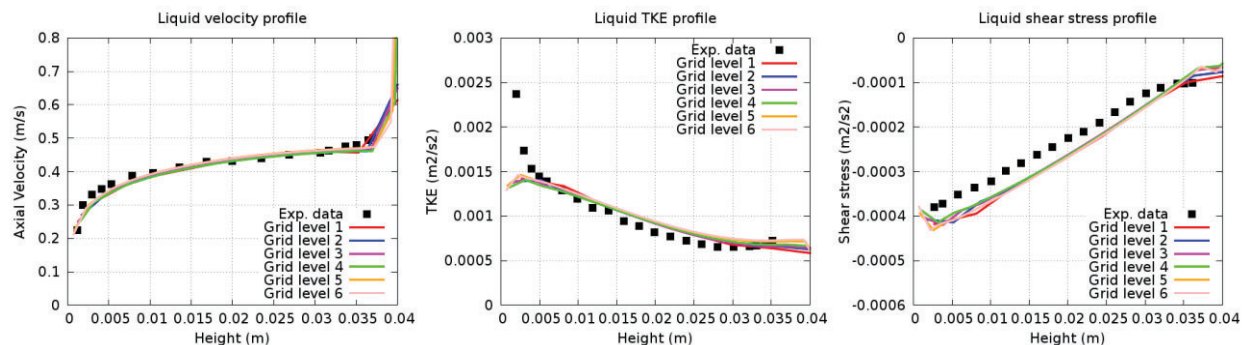
5.2.2. Computational representation

Even if the geometry shape of the experiment allows a 2D computation, an important mean secondary flow has been observed experimentally in the cross-section (in both gas and liquid phases). Therefore, calculations have been done using a 3D computational domain. Six levels of grid have been used (see Table IV). We considered a two-phase, isothermal and turbulent flow (R_{ij}-ε SSG model for both phases), with constant densities and viscosities.

Table IV. Hierarchy of refined meshes for AWST experiment

Grid	Overall number of cells	Number of cells in the water inlet height
Level 1	26 250	7
Level 2	90 508	11
Level 3	225 000	15
Level 4	415 584	18
Level 5	742 500	22
Level 6	1 181 650	26

5.2.3. Results

Figure 8 shows the calculations results and their comparisons with the experimental data. The top (resp. bottom) graphs present liquid (resp. gas) dynamic properties. The mean velocity is shown on the left part, the turbulent kinetic energy profiles are plotted in the middle and the turbulent shear stress on the right part. The bottom axis is directed from the wall to the interface (resp. from the interface to the wall) for the liquid part (resp. gas part). Calculation results (lines) are compared with the experiment (black symbols) for the three mesh refinements.
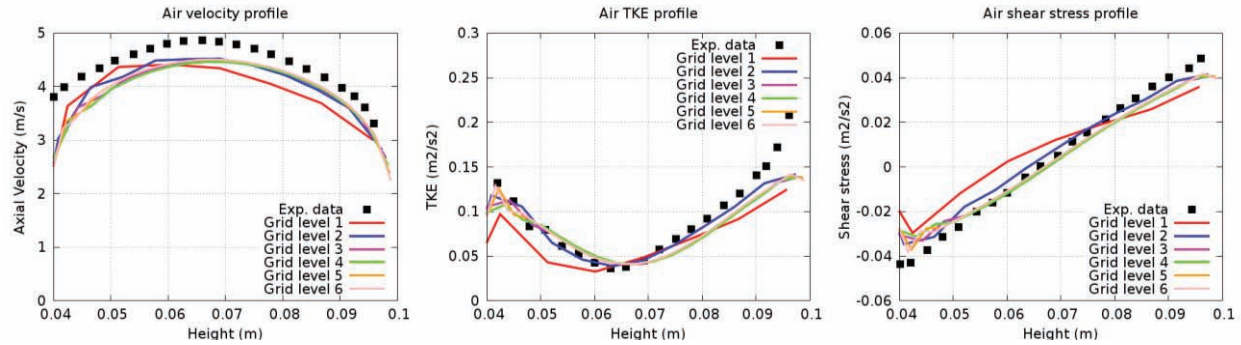
Figure 8. Liquid / air velocity (left), turbulent kinetic energy (middle) and shear stress (right) - comparison between experimental data (symbols) and NEPTUNE_CFD simulations (lines)

Velocity profiles are well predicted for both phases and the turbulent quantities are in good agreement with experimental data. Eventually the agreement and the weak sensitivity to the mesh refinement are satisfactory for a CFD use in a PTS context. In a near future, the run 400 with a wavy free surface and predominant 3D circulations will be investigated to evaluate the contribution of RSM model compared to first order turbulence model.

5.3. Steam / water stratified flows in a channel

5.3.1. Description of the test case

The experimental data are from Chu et al. [24-25]. This experiment deals with a steam / water countercurrent stratified flow. The flow regime of the free surface was observed, it could be smooth or wavy all along the channel. The test section is a circular pipe 2.1 m long, with a diameter of 8.4 cm, slightly inclined (0.2° from the water inlet). The inlet water height is around 2.3 cm. For each case, the measured quantities used for the inlet boundary conditions are the liquid and gas mass flow rates and liquid temperature. Saturated steam is injected and the outlet pressure is the atmospheric one. Eight tests have been selected for the current validation. The first tests from the experiment of 2000 [24] have the lowest inlet flow rates, in which a smooth free surface was observed. Tests from the experiment of 2006 [25] present the highest flow rates, in which a wavy free surface was observed. Only one test case will be presented here, it corresponds to the case with a liquid flow rate of 0.1499 kg/s and a steam flow rate of 0.0049 kg/s. Water is injected at 39.25°C.
The measured quantities used in the comparison with the computations are the liquid temperature and velocity profiles located at 0.6, 1.1, 1.6 and 2.1 m from the water inlet.

5.3.2. Computational representation

Four levels of grid have been used (see Table V). We considered a two-phase, thermal (with large interface) and turbulent flow (R_{ij}-ε SSG model for both phases), with varying properties for both fluids estimated from CATHARE tables. Condensation model is based on the surface divergence model [26].

Table V. Hierarchy of refined meshes for the steam / water experiment

Grid	Overall number of cells	Number of cells in the water inlet height
Level 1	260 120	5
Level 2	725 100	8
Level 3	1 284 500	10
Level 4	2 441 640	13

5.3.3. Results

Figure 9 shows the water temperature and velocity profiles (lines) at different positions in the channel against experimental data (black symbols) for the four refinements.
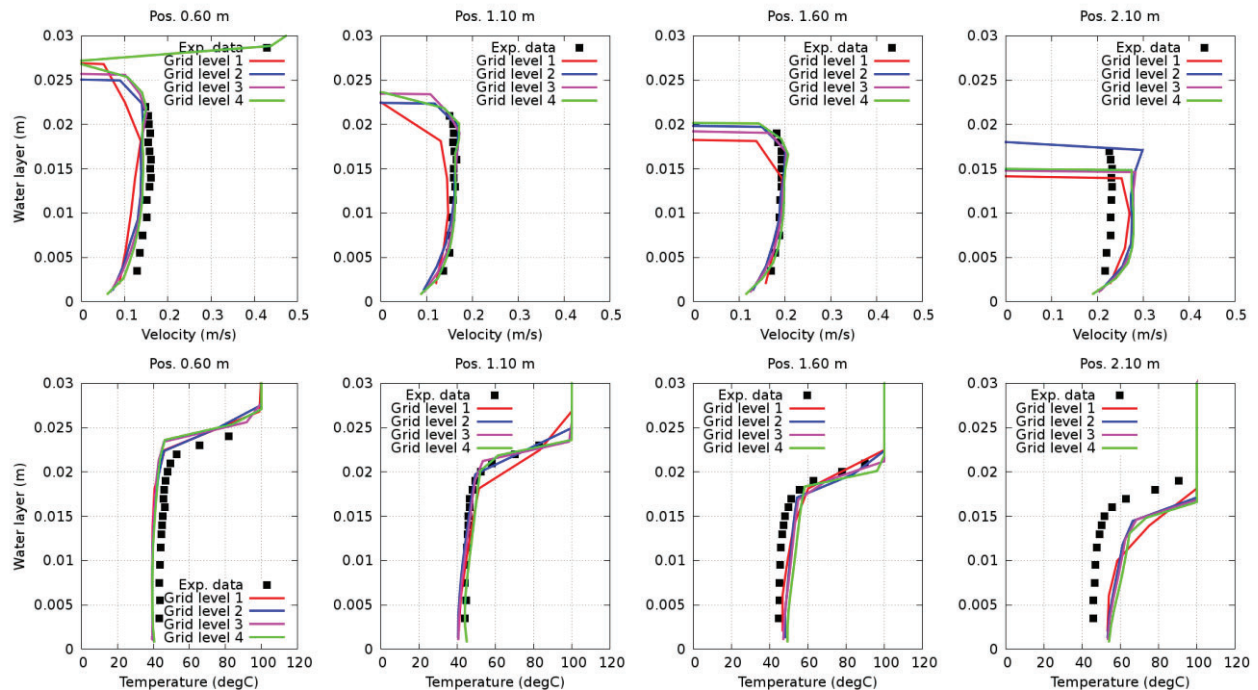

Figure 9. Liquid velocity (top), temperature (bottom) profiles - comparison between experimental data (symbols) and NEPTUNE_CFD simulations (lines)

Velocity and temperature profiles are in good agreement with experimental data, particularly near the water inlet. We can observe some discrepancies when we get closer to the steam inlet. Indeed some uncertainties still remain about the boundary conditions to be used near that inlet to properly model the experiment. Some discussions have been engaged with experimenters to tackle this problem. Eventually the agreement and the weak sensitivity to the mesh refinement are satisfactory.

6. VALIDATION ON INTEGRAL CASES

With the confidence acquired during the previous verification step and validation on separated effects, the following section will now focus on the integral validation of NEPTUNE_CFD, using RSM (R_{ij}-ε SSG) for turbulence prediction and LIM.

6.1. TOPFLOW – PTS experiment

6.1.1. Description of the test case

An important objective of the TOPFLOW-PTS project is the investigation of mixing phenomena inside a cold leg and the downcomer model of a French 900 MWe PWR (at a scale of 1:2.5) during injection of sub-cooled emergency core cooling water [27]. To provide the necessary test data, a special test rig and the peripheral systems were designed and built up in and around the pressure tank of the thermal hydraulic test facility TOPFLOW at Helmholtz-Zentrum Dresden-Rossendorf (HZDR) (see Figure 10). Furthermore, special measurement techniques were developed and commissioned with the test rig where they were implemented, including 112 thermocouples located in the cold leg and 57 in the downcomer.

Probes located in the cold leg are distributed along linear arrays (LA1 to LA4 and 2DA1 to 2DA2, as explained in Figure 10). Other thermocouples are distributed all along the downcomer.
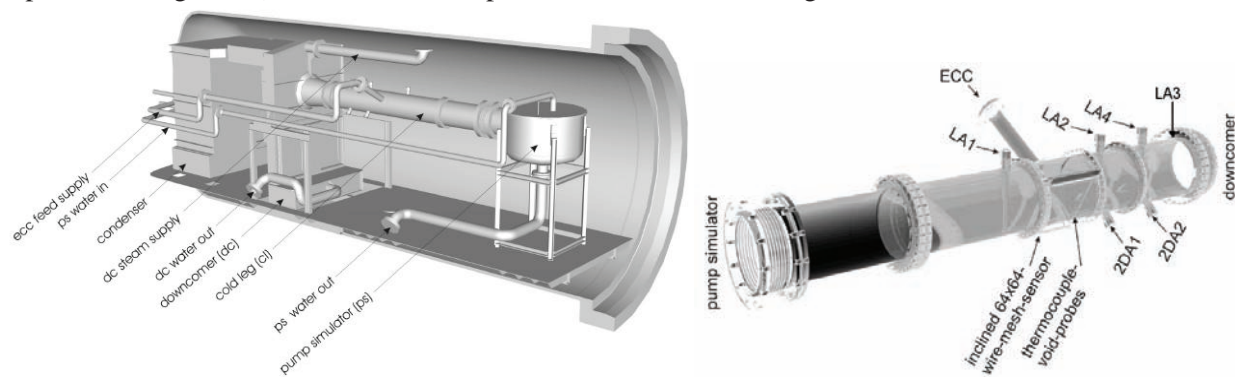

Figure 10. Schematic view of TOPFLOW-PTS experiment (left) and probes positions in the cold leg (right)

Two steam / water cases are presented here. Firstly, a mesh sensitivity study has been done using four different meshes on one steady-state case (3-17) where the water level is set to 50 % of the cold leg diameter and the ECC mass flow rate is constant. Secondly, a transient scenario (3-5) including conjugate heat transfer is presented.

6.1.2. Computational representation

The mesh – including the pump simulator, the cold leg, the ECC and the downcomer – has been generated using Gmsh 2.6.1 [28]. A particular attention has been paid to the mesh quality. The resulting grid is fully hexahedral, without any non-conformity (hanging nodes). The cells characteristic size continuity has also been taken into account to build an as much as possible uniform mesh. The junction between the ECC and the cold leg is totally conforming. A smooth cell's volume progression has been kept to catch the size transition between both tubes. The filleted junction has also been reproduced to avoid a wrong jet computation when the ECC flow is impinging the cold leg [19]. Another important point is to follow the geometry contours with cells of high quality in the boundary layers in order to correctly compute the dynamic and thermal wall functions (see Figure 11).
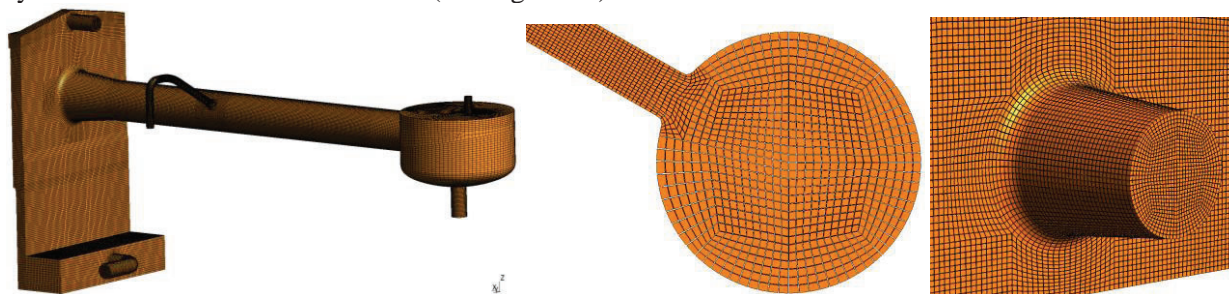

Figure 11. TOPFLOW-PTS mesh (left) – ECC / Cold Leg (middle) – Cold Leg / Downcomer (right)

The same reference mesh (with 778 400 cells) has been used for each case and a sensitivity study has been done with four different refinements (435 422, 778 400, 1 130 378 and 1 768 000 cells) on case 3-17. We considered a two-phase, thermal (with large interface) and turbulent flow (R_{ij}-ε SSG model for both phases), with varying properties for both fluids estimated from CATHARE tables. The condensation model is based on the surface divergence model (Lakehal et al., 2008).

6.1.3. Mesh refinement on a steady-state steam / water case

Temperature profiles obtained with NEPTUNE_CFD (against experimental data) for the 4 arrays in the cold leg are given in Figure 12. Computational data are averaged over the last 60 s of the transient calculation of the steady state.
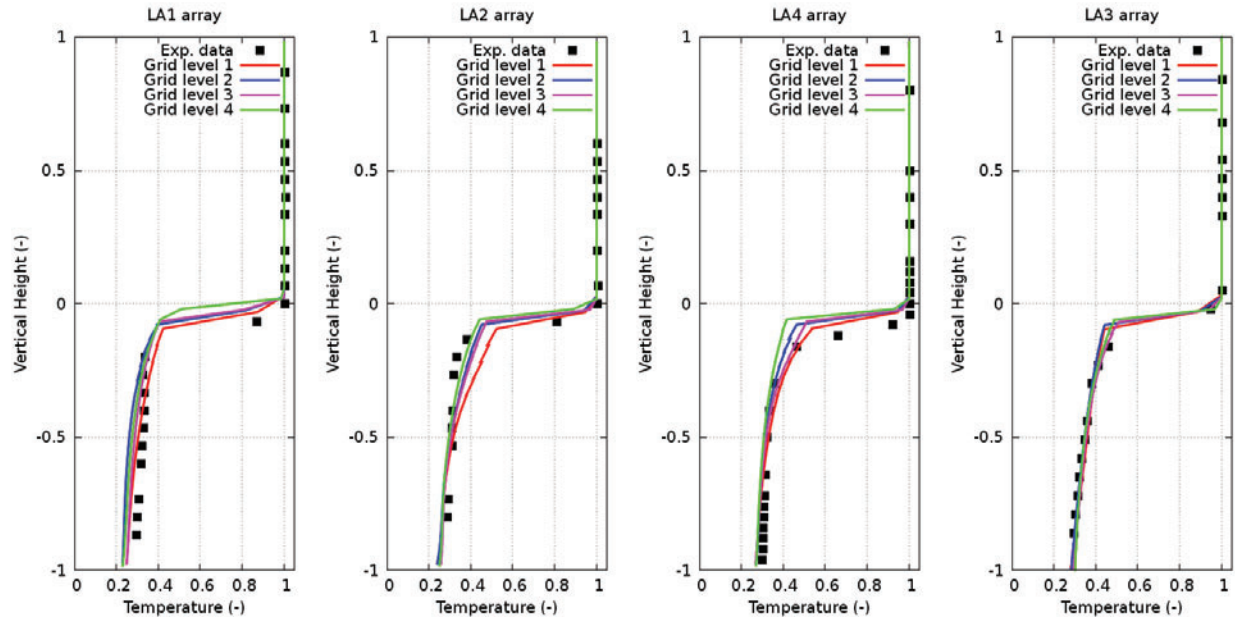

Figure 12. Mesh sensitivity of temperature profile on TOPFLOW-PTS SS-SW 3-17

The global error on the temperature prediction (average of the error on each thermocouple in the liquid phase) and the relative error on the condensation rate prediction (global rate on the whole domain) are given in Table VI.

Table VI. Mesh sensitivity of global temperature and condensation rate prediction

Grid	Global error on the water temperature (averaged over the last 60 s)	Global error on the condensation rate (averaged over the last 20 s)
435 422 cells	3 %	-8 %
778 400 cells	3 %	-8 %
1 130 378 cells	3 %	-3 %
1 768 000 cells	4 %	-5 %

These results show that NEPTUNE_CFD does predict the liquid temperature quite well, no matter the mesh refinement. Regarding the condensation rate, the estimation is slightly varying according to the considered mesh. But we have to keep in mind that experimental condensation rate have been estimated by HZDR with a precision of +/- 25 % - implying that the four predicted rates are in the uncertainty range. Therefore it has been concluded that NEPTUNE_CFD does predict this case quite well without sensitivity to the mesh refinement.

6.1.4. Transient steam / water case with conjugate heat transfer

During the transient scenario, the water level is decreasing until the cold leg is empty. In the same time, the ECC flow temperature decreases slowly. Then, the water level rises again and stabilizes when the cold leg is full with water. During the whole scenario, a rectangular steel plate instrumented with thermocouples is in contact of the water flowing in the downcomer. Consequently, conjugate heat transfer is taken into account by coupling NEPTUNE_CFD with SYRTHES (a thermal code for solid developed

by EDF). The interesting point here is to have a code coupling validation with a scenario representative of a PTS event.

The computation has been performed, based on the reference mesh with 778 400 cells for NEPTUNE_CFD. A comparison between experiment and NEPTUNE_CFD / SYRTHES computation is given in Figure 13. Graphs are representative of the fluid (resp. solid) temperature evolution at a probe located in the water (resp. steel plate) of the downcomer.
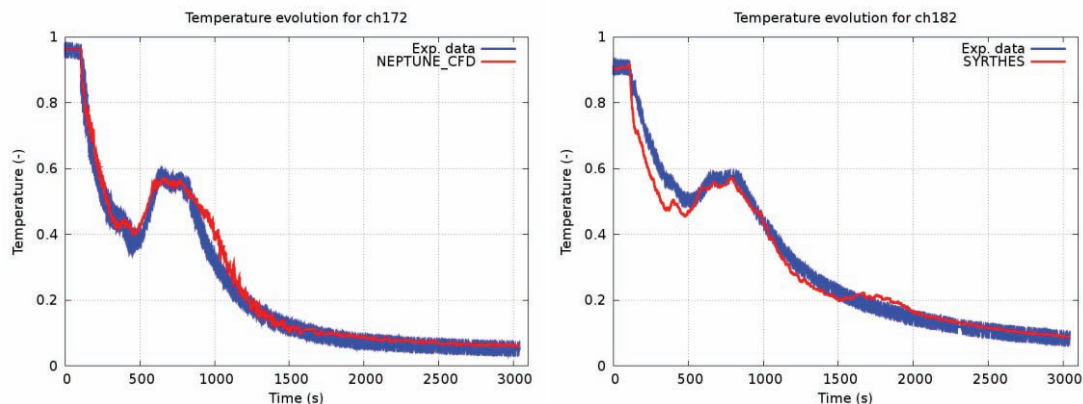

Figure 13. Temperature evolution for the water (left) and the steel (right) – comparison between experimental data (blue line) and simulations (blue line)

The global error on the temperature prediction has been computed for each thermocouple (TC) in the liquid and in the steel plate (Table VII). More precisely, the error is estimated as an average on time periods of 100 s of the difference between experimental and simulation data.

Table VII. Maximum temperature observed for each TC in the fluid and the solid

Max error on the water temperature	Max error on the steel temperature
4 %	13 %

Regarding the modelling of heat conduction in the solid, there is an uncertainty on boundary conditions to be applied to the solid part which is not in contact with the water. From the experimental temperature profiles near the boundaries, we can deduce that there are some heat exchanges between the steel plate and the environment but we are not able to quantify them. As a consequence a null flux condition has been applied on these boundary faces which are not in contact with the fluid. Unfortunately, this boundary condition does induce some discrepancies in the computation because the maximum errors are observed at these points. If we don't consider these thermocouples which are closer to the boundaries, the maximum error on the steel temperature prediction decreases up to 4 %.

Finally, we can say that these results are satisfactory, which is quite encouraging, considering that this transient scenario (with turbulent heat and mass transfer on a complex geometry) is one of the closest validation case to a real PTS event.

7. INDUSTRIAL APPLICATION

From these development and validation feedbacks, a first methodology has been set up to perform future-oriented industrial computations. This section presents the guidelines of this methodology based on NEPTUNE_CFD and SYRTHES coupling – to take into account the conjugate heat transfer between liquid and solid. This methodology must be seen as the result of first attempts to model two-phase PTS in an industrial context and may have to evolve according to the feedback that will be acquired during engineering studies.

7.1. The computing line system

The computing line system is initialised and driven by a first calculation of the PTS scenario with CATHARE (system code). It gives to the CFD code the necessary data regarding the domain initialization, as well as the boundary conditions during the whole transient – pressure and water level in the downcomer, mass flow rates and temperatures for every injection.

The CFD computation (with NEPTUNE_CFD) is based on a fine 3D representation of the interesting zone (fluid domain). It enables to evaluate the fluid temperature at every point of the computational domain. Moreover, the coupling with a thermal code for solid (SYRTHES) gives the temperature evolution within the vessels and legs thickness by taking into account thermal fluid / structure interactions all along the transient scenario.

7.2. Computational domains and meshes

The considered geometry is representative of a French PWR. Two computational domains are considered for this application: the fluid and solid parts (see Figure 14). Generally speaking, the computational domains include the three primary pump scrolls (represented by an equivalent volume), the three cold legs equipped with their ECC and ACCU injections, the whole downcomer and inferior plenum. The hot legs are only modelled by the obstruction they induced in the annular space. A part of the nuclear core is modelled using head losses.
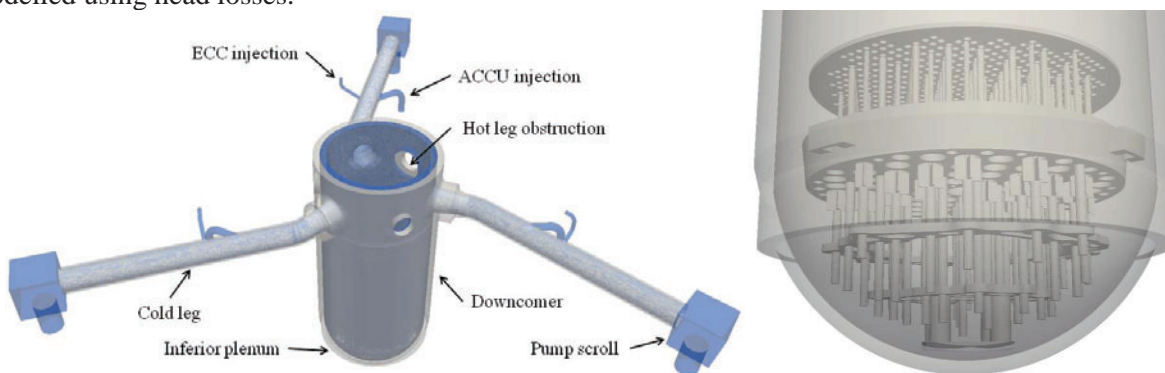

Figure 14. Computational domains representative of a French PWR (fluid domain in blue and solid domain in grey) – zoom on inferior plenum (right)

Mesh characteristics are based on the feedback obtained from the validation step (and mainly on integral cases). Adapting mesh characteristics of these validation cases to this industrial application gives a fluid mesh with about 6 500 000 cells and a solid mesh around 4 000 000 cells. Attention has been paid to the mesh quality, and particularly regarding the criteria described in Part 6.1.2.

7.3. Physical properties and boundary conditions

For both phases (water and steam), physical properties are varying with pressure and temperature. These physical properties are arisen from the CATHARE thermodynamic tables. Regarding steel properties, the density is fixed to a constant value, while the specific heat and thermal conductivity are varying with temperature.

Regarding the boundary conditions for the fluid domain, they are issued from the CATHARE calculation. Water is injected through different inlets to model the ECC and ACCU injections. Some water may also be injected through the U-leg and pump join inlets to model the flow circulation within the primary circuit. The reference pressure is imposed at the top of downcomer. The water level within the downcomer is regulated through the imposed mass flow rate at the outlet located in direction of the superior plenum (see Figure 15).
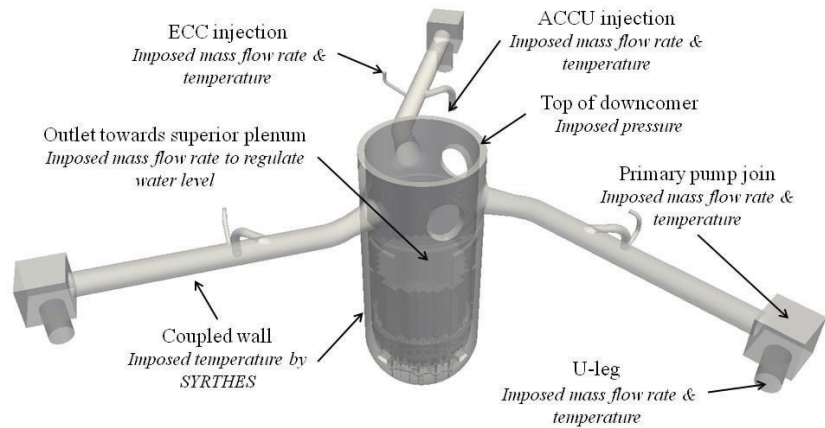
Figure 15. Boundary conditions for the fluid domain

7.4. Results analysis

For the sake of brevity, a qualitative analysis highlighting the main phenomena that can be observed during a two-phase PTS scenario will be given here. Depending on the location within the fluid domain, different physical phenomena occur [29] and are represented by the CFD modelling (cf. Figure 16):

- Zone of free liquid jets (at the outlet of ECC and ACCU injections):
  - Momentum transfer at the jet interface, which could generate instabilities,
  - Condensation at the jet free surface.
- Zone of the impinging jets (in the cold leg, facing the injections):
  - Surface deformation by the jet including generation of waves,
  - Turbulence production below the jet.
- Zone of horizontal flows (in the cold legs):
  - Momentum exchange at the gas-liquid interface including generation of waves,
  - Interfacial heat and mass transfer (steam condensation),
  - Turbulence production at the interface and at the walls,
  - Stratification due to hot and cold water.
- Zone in the downcomer:
  - Interaction of cold flows,
  - Thermal mixing of hot and cold water (buoyancy plume oscillations),
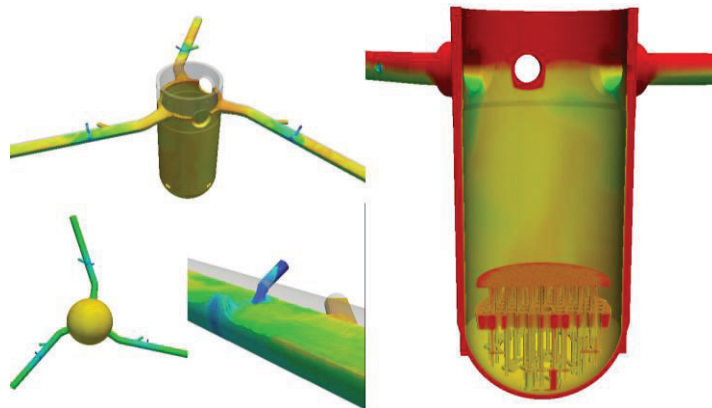 - Heat transfer to the vessel wall.

Figure 16. Industrial application on a French PWR geometry – CFD computation with NEPTUNE_CFD (left) and coupling with thermal code SYRTHES (right)

8. CONCLUSIONS

EDF methodology based on physical analysis, verification, validation and application to industrial scale (V&V), to demonstrate the quality of, and the confidence in results obtained is presented in this paper. It demonstrates that the overall validation of NEPTUNE_CFD 3.0 does cover a great part of the targeted application domain, even if there is still a lack of separated effects validation for the wall heat transfer physical phenomenon – and particularly a lack of experimental reference.

A few verification and validation cases of flows encountered in PTS scenarios have been presented. The same set of models has been applied for every case (LIM with R_{ij}-ε SSG to model turbulence if needed). Even if the BPG [21] advise to include experimental uncertainties in the analysis, the available data in the considered cases in this paper lead to uncertainties which are much smaller than the typical discrepancies between our two-phase CFD calculations and measurements. Therefore this point has not been addressed in this paper. The mesh sensitivity has been investigated on all the test cases (including integral cases). All the experiments deal with free surfaces and in this case, the BPG concede that it is not possible to obtain completely grid-independent results. Nevertheless, a weak sensitivity to the mesh refinement was observed for almost each studied case which gives a lot of confidence in the results presented here.

From these development and validation feedbacks, a methodology has been set up to perform industrial computations. The guidelines of this methodology based on NEPTUNE_CFD and SYRTHES coupling – to take into account the conjugate heat transfer between liquid and solid – has been described. From the analysis of this industrial application, we can conclude that the different expected physical phenomena are well represented by the CFD modelling.

To conclude we can keep in mind that a complete methodology has been defined to model two-phase PTS with NEPTUNE_CFD 3.0. The validation domain of the code being well defined and the weaknesses well known, NEPTUNE_CFD 3.0 may be used to compute quality-controlled PTS applications.

ACKNOWLEDGMENTS

REFERENCES

1. A. Guelfi, D. Bestion, M. Boucker, P. Boudier, P. Fillion, M. Grandotto, J.-M. Hérard, E. Hervieu, P. Péturaud, "NEPTUNE - A New Software Platform for Advanced Nuclear Thermal-Hydraulics", *Nuclear Science and Engineering,* **156**, pp 281-324 (2007).
2. B. Gaudron, H. Cordier, S. Bellet, D. Monfort, "Using the PIRT to Represent Application and Validation Domains for CFD Studies", *Proceedings of CFD4NRS-5,* Zurich, 9-11 September 2014.
3. M. Ishii, *Thermo-fluid Dynamics Theory of Two-Phase Flow,* Eyrolles, Collection de la direction des Etudes et recherches d'Electricité de France (1975).
4. J.-M. Delhaye, M. Giot, M.L. Riethmuller, *Thermal-hydraulics of two-phase systems for industrial design and nuclear engineering*, Hemisphere and McGraw Hill (1981).
5. N. Méchitoua et al., "An unstructured finite volume solver for two-phase water/vapor flows modelling based on an elliptic-oriented fractional step method", *Proceedings of NURETH-10,* Seoul, 5-9 October 2003.
6. S. Mimouni, F. Archambeau, M. Boucker, J. Laviéville, C. Morel, "A second order turbulence model based on a Reynolds stress approach for two-phase boiling flow. Part 1: Application to the ASU-annular channel case", *Nuclear Engineering and Design,* (2009).

7. S. Mimouni, F. Archambeau, M. Boucker, J. Laviéville, C. Morel, "A second order turbulence model based on a Reynolds stress approach for two-phase boiling flow. Part 1: Adiabatic cases", *Science and Technology of Nuclear Installations,* **792395**, 14 (2009).

8. P. Coste, "A Large Interface Model for two-phase CFD", *Nuclear Engineering and Design,* **255**, pp. 38-50 (2013).

9. J. Laviéville, P. Coste, "Numerical modeling of liquid-gas stratified flows using two-phase Eulerian approach", *Proceedings of the 5ᵗʰ International Symposium on Finite Volumes for Complex Applications,* Aussois, 8-13 June 2008.

10. P. Coste, J. Pouvreau, C. Morel, J. Laviéville, M. Boucker, A. Martin, "Modeling turbulence and friction around a large interface in a three-dimension two-velocity eulerian code", *Proceedings of NURETH-12,* Pittsburgh, 30 September - 4 October 2007.

11. P. Coste, J. Pouvreau, J. Laviéville, M. Boucker, "A two-phase CFD approach to the PTS problem evaluated on COSI experiment", *Proc. ICONE 16,* Orlando, 11-15 May 2008.

12. P. Coste , J. Laviéville, "A Wall Function-Like Approach for-Two-Phase CFD Condensation Modeling of the Pressurized Thermal Shock", *Proceedings of NURETH-13,* Kanazawa, 27 September - 2 October 2009.

13. B.E. Launder, D.B. Spalding, "The numerical computation of turbulent flows", *Computer Methods in Applied Mechanics and Engineering*, **3**, pp. 269-289 (1974).

14. V. Guimet, D. Laurence, "A linearised turbulent production in the k-ε model for engineering applications", *Proceedings of the 5th international symposium on engineering turbulence modelling and measurements*, Mallorca, September 2002.

15. C.G. Speziale, S. Sarkar, T.B. Gatski, "Modelling the pressure-strain correlation of turbulence: an invariant dynamical systems approach", *J. Fluid Mechanics,* **227**, pp. 245-272 (1991).

16. S. Mimouni, F. Archambeau, M. Boucker, J. Laviéville, C. Morel, "A second order turbulence model based on a Reynolds stress approach for two-phase boiling flow and application to fuel assembly analysis", *Nuclear Engineering and Design,* **240**, pp. 2225-2232 (2010).

17. P. Coste, J. Laviéville, "A Turbulence Model for Large Interfaces in High-Reynolds Two-Phase CFD", *Nuclear Engineering and Design,* **284**, pp. 162-175 (2015).

18. N. Mérigoux, J. Laviéville, S. Mimouni, M. Guingo, C. Baudry, "Reynolds Stress Turbulence Model applied to Two-Phase Pressurized Thermal Shocks in Nuclear Power Plant", *Proceedings of CFD4NRS-5,* Zurich, 9-11 September 2014.

19. P. Coste, N. Mérigoux, "Two-phase CFD validation: TOPFLOW-PTS Steady-State Steam-Water tests 3-16, 3-17, 3-18, 3-19", *Proceedings of CFD4NRS-5,* Zurich, 9-11 September 2014.

20. NRC, *Transient and accident analysis methods*, NRC Regulatory guide 1.203 (2005).

21. OECD, "Best Practice Guidelines for the Use of CFD in Nuclear Safety Applications - Revision"*, OECD Nuclear Energy Agency,* Technical Report NEA/CSNI/R(2014)11.

22. K. M. T. Kleefsman, G. Fekken, A. E. P Veldman, B. Iwanowski, and B. Buchner, "A Volume-Of-Fluid based simulation method for wave impact problem", *J. Computational Physics*, **206**, pp. 363-393 (2005).

23. J. Fabre, L. Masbernat, C. Suzanne, "Stratified Flow, Part I: Local Structure", *Multiphase Science and Technology*, **3**, pp. 285-301 (1987).

24. I-C. Chu, M-K. Chung, S-O. Yu, M-H. Chun, "Interfacial Condensation Heat Transfer for Countercurrent Steam-Water Stratified Flow in a Circular Pipe", *J. of the Korean Nuclear Society,* **32**, pp. 142-156 (2000).

25. K-W. Lee, I-C. Chu, S-O. Yu, H-C. No, "Interfacial Condensation for Countercurrent Steam-Water Stratified Flow Wavy Flow in a Horizontal Circular Pipe", *Int. J. of Heat and Mass Transfer,* **49**, pp. 3121-3129 (2006).

26. D. Lakehal, M. Fulgosi, G. Yadigaroglu, "Direct numerical simulation of condensing stratified flow", *J. Heat Transfer,* **130**, 021501 (2008).

27. P. Péturaud et al., "General overview of the TOPFLOW-PTS experimental program", *Proceedings of NURETH-14,* Toronto, 25-30 September 2011.

28. C. Geuzaine, J.-F. Remacle, "Gmsh: a three-dimensional finite element mesh generator with built-in pre- and post-processing facilities"*, Int. J. Numerical Methods in Engineering*, **79**, pp. 1309-1331 (2009).

29. D. Bestion et al., "Extension of CFD codes to Two-phase Flow Safety Problems", *OECD Nuclear Energy Agency*, Technical Report NEA/SEN/SIN/AMA(2006)2.